Stability Analysis of Radial Jet Drilling in Chalk Reservoirs

Medetbekova M.K.,[1] Salimzadeh S., Ph.D., [2] Christensen H.F, [3] and Nick H.M., Ph.D.[4]

[1]Centre for Oil and Gas, Technical University of Denmark, P.O. Box 2800, Kgs. Lyngby, B 375, e-mail: maiyam@dtu.dk
[2]Centre for Oil and Gas, Technical University of Denmark, P.O. Box 2800, Kgs. Lyngby, B 375, e-mail: saeeds@dtu.dk
[3]Geo, P.O. Box 2800, Kgs. Lyngby, Maglebjergvej 1, e-mail: hfc@geo.dk
[4]Centre for Oil and Gas, Technical University of Denmark, P.O. Box 2800, Kgs. Lyngby, B 375, e-mail: hamid@dtu.dk

ABSTRACT

In this work, the stability of Radial Jet Drilled (RJD) laterals in both injection and production wells are studied. Thermo-elastoplastic and poro-elastoplastic finite element models are developed in a robust software (ABAQUS) and used to simulate the injector and producer laterals. Several cases with varying in situ stresses are considered. The temperature and pressure gradients of 60°C and 10 MPa are applied. The simulation results show that both hydraulic and thermal stresses can affect the stability of a lateral by increasing the plastic region near the lateral. The thermal effect increases the plastic region around the producer, while the hydraulic effect increases the plastic region and its magnitude at the producer.

Keywords: Poro-elastoplasticity, Thermo-elastoplasticity, Radial jet drilling, Chalk reservoir

INTRODUCTION

Radial Jet Drilling (RJD) is an economically feasible productivity enhancement technique that uses hydraulic jet energy of fluids to drill lateral holes. The laterals can be drilled relatively fast, penetrating up to 100-200m, in up to 16 directions from the existing well shafts (Kamel, 2014). RJD has become a very attractive well stimulation candidate for both hydrocarbon reservoirs (Buset et al., 2001; Kamel, 2014), and geothermal systems (Peters et al, 2015). There are few successful documented cases of application of RJD method in the petroleum industry. Observations from field cases show that after implementing RJDs, the production increases significantly shortly after jetting, but it is susceptible to reduction in the long term. This may occur due to instability of the jetted holes. Therefore, RJDs are expected to have a limited life time (Ragab, 2013; Peters et al, 2015).

Present day, more than 80% of the hydrocarbon production in the Danish part of the North Sea comes from chalk reservoirs of Maastrichtian and Danian ages (Abramovitz, 2008). In the Halfdan field, located in southern Danish North Sea, the reservoir comprises of unfractured, low permeability chalk (0.5-2.0 mD) of mainly Maastrichtian age. In the Upper Maastrichtian, the average porosity can have values of 25-30%, whereas a sharp decrease in porosity to about 10-15% is observed in the Lower Maastrichtian to Campanian layers (Albrechtsen at el., 2001). Data from 4D seismic survey and reservoir modelling in conjunction with the production and geologic data suggest that there might be unswept areas in the deep reservoir layers (Calvert et al., 2014). RJD technique is considered as a potential method for accessing the unswept areas and improving oil recovery.

Well instability occurs when the stress state exceeds the rock strength. Also, the temperature and pressure gradients around the well further affect the axial and tangential stresses around an open hole (Fjær et al., 2008). In case of a RJD, the stability issues can be more profound due to the lacking of support from a casing. The instability of a RJD in chalk can be even more severe due to the fines production, hydraulic fracture formation as well as plastic deformation of the rock. Therefore, a comprehensive study is required in order to mitigate the hole collapse issues and to prolong the service of the lateral. The objective of the present work is to evaluate i) how thermally induced stresses affect the lateral stability; ii) how pore pressure gradients affects the stability of the lateral in production and injection wells. For this purpose, coupled thermo-elastoplastic and poro-elastoplastic numerical models are implemented in a robust finite element (FE) code, Abaqus. Abaqus provides possibilities of modelling coupled thermal-hydro-mechanical analysis.

GOVERNING EQUATIONS

Poro- and Thermo-elastoplastic models. For a given elementary volume, at quasi-static conditions, the equilibrium equation can be written as

$$\text{div}\,\boldsymbol{\sigma} + \mathbf{F} = 0 \tag{1}$$

where $\boldsymbol{\sigma}$ is the total stress and $\mathbf{F}$ is the body force per unit volume. In general, the effective stress for the fluid-saturated rock is defined as (Biot, 1941)

$$\boldsymbol{\sigma}' = \boldsymbol{\sigma} + \alpha p \mathbf{I} \tag{2}$$

where $\boldsymbol{\sigma}'$ is the effective stress, α is the Biot coefficient, p is the fluid pressure in the rock, $\mathbf{I}$ is the second order identity tensor. The Biot coefficient may be estimated from:

$$\alpha = 1 - \frac{K}{K_s} \tag{3}$$

where K is the bulk modulus of a rock matrix and K_s is the bulk modulus of the solid grains (Zimmerman, 2000). The stress-strain relationship for poroelasticity can be written as

$$\boldsymbol{\sigma}' = \mathbf{D}^e \boldsymbol{\varepsilon}^e \tag{4}$$

in which $\mathbf{D}^e$ is the drained stiffness matrix, and $\boldsymbol{\varepsilon}^e$ is the elastic strain tensor defined as

$$\boldsymbol{\varepsilon}^e = \boldsymbol{\varepsilon} - \boldsymbol{\varepsilon}^p \tag{5}$$

where, $\boldsymbol{\varepsilon}$ and $\boldsymbol{\varepsilon}^e$ are the total and plastic strain tensors, respectively. Under infinitesimal deformation assumption, strain-displacement relation is given by

$$\boldsymbol{\varepsilon} = \frac{1}{2}(\nabla\mathbf{u} + \nabla\mathbf{u}^T) \tag{6}$$

where $\mathbf{u}$ is the displacement vector of the rock solid. Combining equations 1-4, the governing differential equation for poroelastic medium can be written as

$$\mathrm{div}(\mathbf{D}^e\boldsymbol{\varepsilon}^e - \alpha p\mathbf{I}) + \mathbf{F} = 0 \tag{7}$$

In a thermoelastic medium, when temperature change occurs from an initial temperature T_0 to a new value T, under the assumption of linearity, the thermal strains in the solid rock may be written (Zimmerman, 2000)

$$\boldsymbol{\varepsilon}_T = -\boldsymbol{\beta}(\mathrm{T} - T_0) \tag{8}$$

where $\boldsymbol{\beta}$ is the thermal expansivity tensor of the rock. The stress-strain relationship for thermoelasticity we may write as (Khalili and Selvadurai, 2003)

$$\boldsymbol{\sigma} = \mathbf{D}^e\boldsymbol{\varepsilon}^e - \boldsymbol{\beta}K(\mathrm{T} - T_0)\mathbf{I} \tag{9}$$

Combining Eq. 8 with Eq. 1 gives the governing differential equation for a thermoelastic medium as

$$\mathrm{div}(\mathbf{D}^e\boldsymbol{\varepsilon}^e - \beta_m K(T_m - T_{m0})\mathbf{I}) + \mathbf{F} = 0 \tag{10}$$

Plasticity model. For representing inelastic behavior, a Concrete Damaged Plasticity (CDP) model has been chosen, which uses concepts of isotropic damaged elasticity in combination with isotropic compressive and tensile plasticity. This model is based on the models proposed by Lubliner et al. (1989) and by Lee and Fenves (1998). For this paper, only the plasticity part of the model has been used, and using the damage part is still under investigation. The model uses a yield condition that account for different evolution of strength under tension and compression. In terms of effective stresses the yield function takes the form

$$F(\sigma', \varepsilon^{pl}) = \frac{1}{1-\chi}\left(q - 3\chi p + \mathrm{ɣ}\varepsilon^{pl}(\sigma'_{max}) - \Upsilon(\sigma'_{max})\right) - \sigma'_c\left(\varepsilon_c^{pl}\right) \leq 0, \tag{11}$$

where

$$\chi = \frac{\left(\frac{\sigma_{bo}}{\sigma_{co}}\right)-1}{2\left(\frac{\sigma_{bo}}{\sigma_{co}}\right)-1},\ 0 \leq \chi \leq 0.5,\ \mathrm{ɣ} = \frac{\sigma'_c\left(\varepsilon_c^{pl}\right)}{\sigma'_t\left(\varepsilon_t^{pl}\right)}(1-\chi) - (1+\chi);\ \Upsilon = \frac{3(1-k_c)}{2k_c-1} \tag{12}$$

χ and Υ are dimensionless material constants; p is effective hydrostatic pressure; q is the Mises equivalent effective stress; σ_{bo}/σ_{co} is the ratio between the limit of bi-axial compression and that of uniaxial compression (default value is 1.16); k_c is the ratio between the second invariant of the stress tensor at the tensile meridian and the second invariant at the compressive meridian under arbitrary pressure, it is required that $0.5 < k_c \leq 1.0$, with a default value as 0.66; σ'_c and σ'_t is the effective compressive and tensile strength respectively. The non-associated plastic flow rule is adopted in the model. The plastic potential G is in the form of Drucker-Prager type and is expressed as:

$$G = ((\epsilon\sigma_{t0}\, tan\psi)^2 + q^2)^{\frac{1}{2}} - ptan\psi \quad (13)$$

where ψ is the dilatancy angle, σ_{t0} is the uniaxial tensile stress at failure, ϵ is a model parameter referred to as the eccentricity, that defines the rate at which the function approaches the asymptote (default value is 0.1) (Dassault Systèmes, 2014).

METHODS

Model description and validation. The FE model geometry consists of a lateral hole drilled from a vertical well and its surrounding formation. A 2D model is created assuming plane-strain behaviour. The cross-section of a jetted lateral varies between a star shape and a circular shape. Several parameters can affect the shape of the hole such as the magnitude of the in situ stress, drilling fluid chemistry, and the number of nozzles on the drilling cone. Bi et al. (2014) studied the effect of number of jetting bit holes on the shape of the erosion hole. Their experimental results show that the form of drilled hole becomes more round with the increase of holes on the jet bit. Also, higher *in situ* stresses and acid injection can create a round lateral shape. In the present study, the hole is assumed to be circular. Figure 1a shows the setup of the model. Horizontal red line a-b shows the path along which the data is collected from the nodes for the plots. The radius of the hole is 0.0254 m. An unstructured mesh with quadratic elements is used, with total 6274 elements. The validity of the mesh size is tested in comparison with the analytical solution for the horizontal and vertical stresses distribution around a hole, as shown in Figure 1b. The compression test plot used in the model is given in Figure 1c. The rock and the fluid's physical properties used in the model are listed in Table 1.

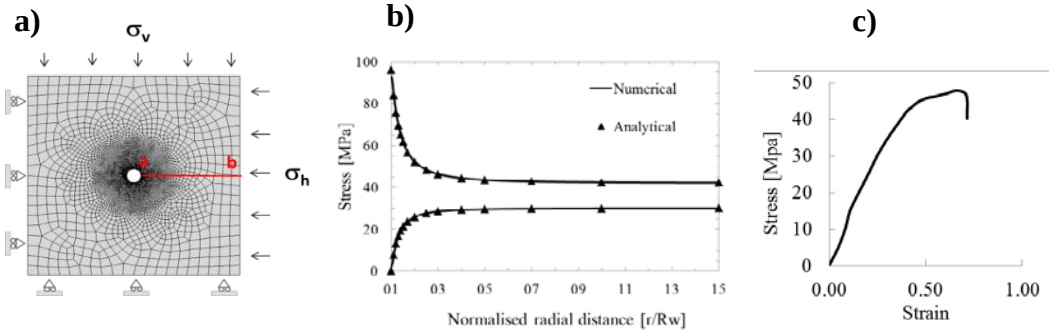

Figure 1. a) Set-up of the 2D numerical model; b) Horizontal and vertical stress distribution, a linear elastic formation is subjected to anisotropic loading (σ_v= 42MPa, σ_h = 30MPa); c) Compression test plot.

The numerical analysis consists of two models: Thermo-elastoplastic and poro-elastoplastic models. The temperature at the lateral's wall is set to 20°C, while the host rock has an initial temperature of 80°C, and compared with constant temperature distribution of 80°C across the whole model domain. In the poro-elastoplastic model, the effect of fluid pressure gradient of

10 MPa on the stability of the hole is examined in both injection and production wells. The heat and flow equations are solved for steady-state.

Table 1. Rock properties used in the model.

Parameters	Value	Parameters	Value
Young's modulus, MPa	13214	Thermal conductivity, W/(m K)	2.07
Poisson's ratio	0.2	Expansion coefficient, $°C^{-1}$	1.65×10^{-5}
Dilatancy angle	15	Specific heat capacity, J/(kg K)	900
Flow potential eccentricity	0.1	Compressive yield stress, MPa	37-48
σ_{bo}/σ_{co}	1.16	Compressive inelastic strain	0-0.004373
k_c	0.66	Tensile yield stress, MPa	0.5-2
Viscosity parameter	0	Tensile inelastic strain	0-0.0036
Bulk density, kg/m^3	1700	Porosity, %	24

RESULTS AND DISCUSSION

Coupled thermo-elastoplastic analysis. The effect of temperature on the distribution of horizontal and vertical stress around the hole with and without variation of temperature across the domain is presented in Figure 2. In this analysis, simulation was performed with varying vertical stress (30, 35, 42 MPa) and temperature gradient (dT=60°C and dT=0°C), while the horizontal stress kept at constant value of 30 MPa.

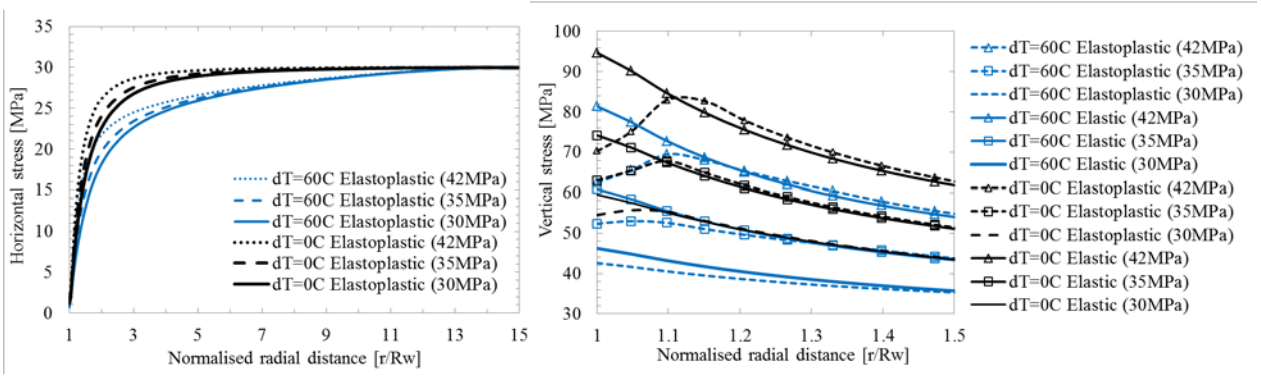

Figure 2. Horizontal and vertical stress distributions in the thermo-elastoplastic and thermo-elastic models.

In Figure 2, the horizontal stress along the line a-b is presented for different cases. Injection of cold fluid results in the contraction of the rock around the injection well, and so the horizontal stress is reducing for the non-isothermal cases. Also, in Figure 2, higher vertical stress is observed at the boundary of the lateral for the elastic cases. When the plastic deformation is allowed, the stresses at the vicinity of the hole are reduced due to the plastic deformation. In addition, when the effect of temperature reduction is added, the vertical stress in the vicinity of the hole further reduces due to the contraction of the rock. At the hole's wall the maximum plastic strain reduces in the non-isothermal cases due to contraction of the medium. The cooling of the chalk around the

hole causes redistribution of stresses which increases the plastic deformations as we move away from the wall. The redistribution of stresses in the non-isothermal cases also causes plastic deformation at the crown (top of the hole) while in isothermal cases no plastic deformation is observed at this point as shown in Figure 3. Furthermore, the yielding of the chalk around the hole causes redistribution of stresses and that increases the vertical stress at a normalised distance larger than 1.1 for the 42 MPa vertical stress case.

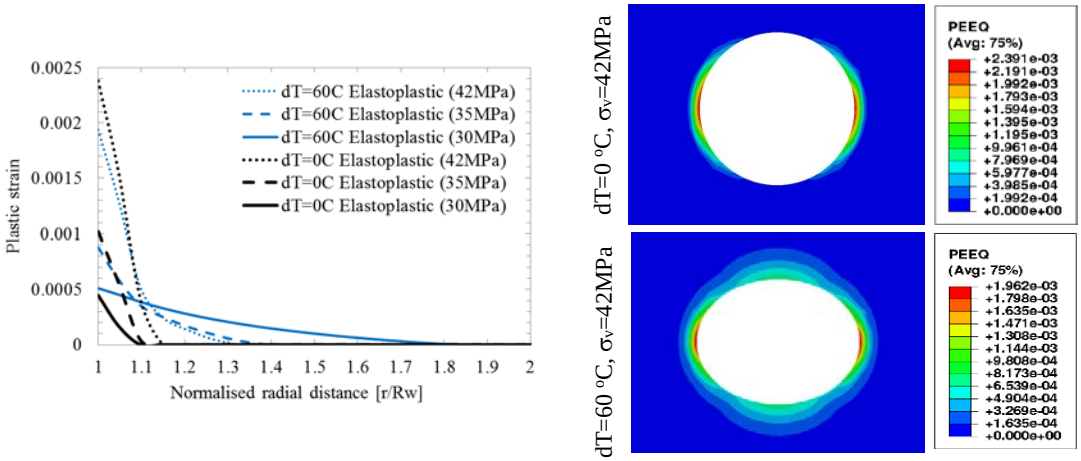

Figure 3. Plastic strain distribution in the vicinity of the lateral. The contours are presented for the case of σ_v = 42 MPa.

Coupled poro-elastoplastic analysis. Another set of analysis is done to define the effect of the fluid pressure gradient on the stability of the hole. Simulations are carried for both production and injection wells using a pressure gradient of 10 MPa. Again, the applied vertical stress is varied between 30, 35 and 42 MPa, while the horizontal stress remains constant and is equal to 30 MPa. The porous medium is considered fully saturated with water.

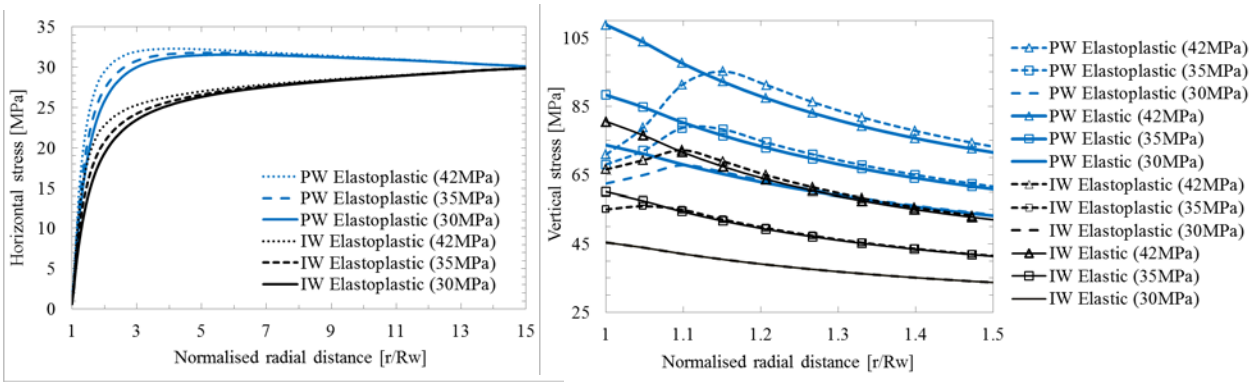

Figure 4. Horizontal and vertical stress distributions in the poro-elastoplastic and poro-elastic models.

Horizontal and vertical stress distributions are shown for production and injection cases in elastic and elastoplastic medium in Figure 4. When fluid is injected into the lateral, the pore pressure rises in the surroundings of the lateral, thereby reducing effective stress in the system. In

the production well, on the other hand, pore pressure drawdown increases the effective stress. The higher and lower stresses around the producer and injector laterals are observed in our simulations as shown in Figure 4. When plastic deformation is allowed, plastic strains develop around the lateral, and that reduces the vertical stress in both injector and producer. The plastic deformation further redistributes the stresses so that the vertical stress for the 42 MPa case, for instance, is higher in the elastoplastic model than the elastic one at normalised radial distance larger than 1.15. Also, higher plastic strains are observed in the producer compared to the injector, shown in Figure 5.

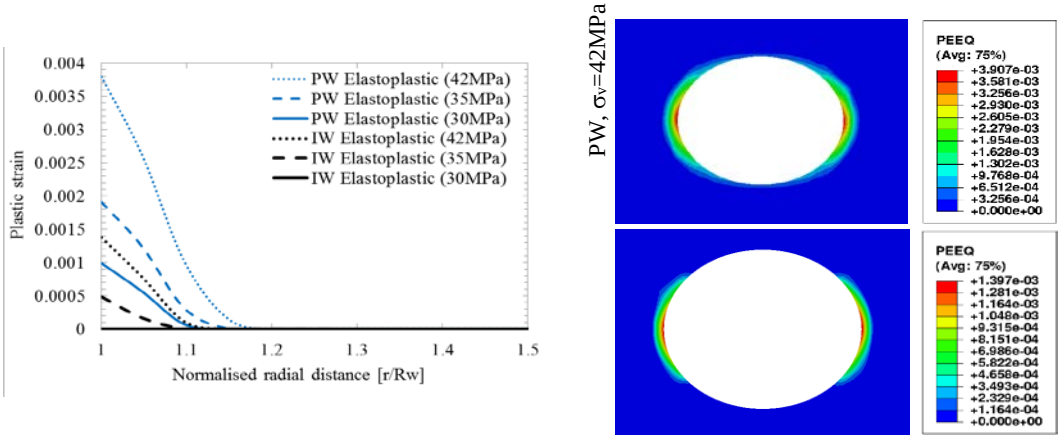

Figure 5. Plastic strain distribution in the vicinity of the lateral. The contours are presented for the case of σ_v = 42 MPa.

CONCLUSION

The stability of a RJD lateral in chalk reservoirs is investigated using thermo-elastoplastic and poro-elastoplastic finite element models. The magnitude and spatial distribution of the plastic strain is used as a measure for the stability of a lateral injector and producer. Based on this criterion, the simulation results show that both hydraulic and thermal stresses affect the stability of a lateral. The thermal effect increases the plastic region around the producer, while the hydraulic effect increases the plastic region and its magnitude at the producer. Therefore, the highest plastic strain is observed in the lateral located at the producer. These results are consistent with the field observations where the laterals at the producer have a short lifetime. This is an ongoing research

and developing a fully coupled thermo-hydro-mechanical model that incorporates mechanical damage is in process.

ACKNOWLEDGMENTS

This project has received funding from the European Union's Horizon 2020 research and innovation programme under grant agreement No 654662 as well as the Danish Hydrocarbon Research and Technology Centre under the Advanced Water Flooding programme.

REFERENCES

Abramovitz, T. (2008). *Geological Survey of Denmark and Greenland Bulletin*. 15, 17–20.

Albrechtsen, T, Andersen, S.J, Dons, T, Engstrøm, F, Jørgensen, O & Sørensen, F.W. (2001). "Halfdan: Developing Non-Structurally Trapped Oil in North Sea Chalk". SPE 71322.

Bi G., Li G., Shen Zh., Huang Zh., Yang R.(2014). "Design and Rock Breaking Characteristic Analysis of Multi-jet Bit on Radial Horizontal Drilling". *Proceedings*, 2014-3. DOI: 10.5510/OGP20140300206.

Buset, P., Riiber, M., Eek, A. (2001). "Jet Drilling Tool: Cost-Effective Lateral Drilling Technology for Enhanced Oil Recovery". SPE/ICoTA Coiled Tubing Roundtable, Houston, Texas, 7-8 March.

Biot, M.A. (1941). "General theory of three dimensional consolidation". *Journal of Applied Physics*. 12: 155–164.

Calvert, M. A. Vagg, L. D. , Lafond, K. B., Hoover, A. R., Ooi, K. C., Herbert, I. H. (2014). "Insights into sweep efficiency using 4D seismic at Halfdan field in the North Sea". *The Leading Edge*, 33(2), 182–187. DOI: 10.1190/tle33020182.1.

Dassault Systèmes. (2014). "ABAQUS® User Manual (version 6.14)". SIMULIA, a division of Dassault Systèmes, Providence, RI, USA.

Fjær, E., Holt, R.M., Horsrud, P., Raaen, A.M., Risnes, R. (2008). "Petroleum related rock mechanics". 2nd edition. *Developments in Petroleum Science, Elsevier*. ISBN: 978-0-444-50260-5/ISSN: 0376-7361.

Kamel, A.H. (2014). "RJD revitalizes mature Kansas oilfield". *Oil & Gas Journal*, 112(10).

Khalili, N., Selvadurai, A. P. S. (2003). "A fully coupled constitutive model for thermo-hydro-mechanical analysis in elastic media with double porosity". *Geophysical Research Letters*. DOI: 10.1029/2003GL018838.

Lee, J., & G. L. Fenves. (1998b)."A plastic-damage concrete model for earthquake analysis of dams". *Earthquake Engineering and Structural Dynamics*, v. 27, no. 9, p. 937–956, DOI:10.1002/(SICI)1096-9845(199809)27: 9<937::AID-EQE764>3.0.CO;2-5.

Lubliner, J., J. Oliver, S. Oller, and E. Oñate. (1989). "A plasticdamage model for concrete". *International Journal of Solids and Structures*, v. 25, no. 3, p. 299–326, DOI:10.1016/0020-7683(89)90050-4.

Peters, E., Veldkamp, J.G., Pluymaekers, M.P.D., Wilschut, F. (2015). "Radial drilling for Dutch geothermal Applications". TNO 2015 R10799.

Ragab, A. (2013). "Improving well productivity in an Egyptian oil field using radial drilling

technique". *Journal of Petroleum and Gas Engineering*, vol. 4(5), 103-117 pp, DOI 10.5897/JPGE2013.015.

Zimmerman, R.W., 2000. "Coupling in poroelasticity and thermoelasticity". *International Journal of Rock Mechanics & Mining Sciences* 37: 79-87.